METFORMIN LOWERS PLASMA TRIGLYCERIDES BY PROMOTING VLDL-TRIGLYCERIDE CLEARANCE BY BROWN ADIPOSE TISSUE IN MICE

MARIËTTE R. BOON*
JANINE J. GEERLING*
GERARD C. VAN DER ZON
SJOERD A.A. VAN DEN BERG
ANITA M. VAN DEN HOEK
MARC LOMBÈS
HANS M.G. PRINCEN
LOUIS M. HAVEKES
PATRICK C.N. RENSEN
BRUNO GUIGAS

* Both authors contributed equally

Diabetes 2014; 63: 1-12.

ABSTRACT

Metformin is the first-line drug for the treatment of type 2 diabetes. Besides its well-characterized antihyperglycemic properties, metformin also lowers plasma VLDL triglycerides (TGs). In this study, we investigated the underlying mechanisms in APOE*3-Leiden.CETP mice, a well-established model for human-like lipoprotein metabolism. We found that metformin markedly lowered plasma total cholesterol and TG levels, an effect mostly due to a decrease in VLDL-TG, whereas HDL was slightly increased. Strikingly, metformin did not affect hepatic VLDL-TG production, VLDL particle composition, and hepatic lipid composition but selectively enhanced clearance of glycerol tri[3H] oleate-labeled VLDL-like emulsion particles into brown adipose tissue (BAT). BAT mass and lipid droplet content were reduced in metformin-treated mice, pointing to increased BAT activation. In addition, both AMP-activated protein kinase α1 (AMPKα1) expression and activity and HSL and mitochondrial content were increased in BAT. Furthermore, therapeutic concentrations of metformin increased AMPK and HSL activities and promoted lipolysis in T37i differentiated brown adipocytes. Collectively, our results identify BAT as an important player in the TG-lowering effect of metformin by enhancing VLDL-TG uptake, intracellular TG lipolysis, and subsequent mitochondrial fatty acid oxidation. Targeting BAT might therefore be considered as a future therapeutic strategy for the treatment of dyslipidemia.

INTRODUCTION

Metformin is one of the most widely used glucose-lowering agents for the treatment of type 2 diabetes (1) and is now considered the first-line drug therapy for patients (2). This antidiabetic drug from the biguanides family is prescribed for its effective antihyperglycemic action, mostly achieved through a potent reduction of hepatic glucose production secondary to inhibition of gluconeogenesis (3). Interestingly, another important but often overlooked property of metformin relies on its beneficial. effect on the blood lipid profile, which is characterized by a significant reduction in circulating triglycerides (TGs) and VLDL cholesterol and increased HDL cholesterol levels (4). This metabolic feature might partly be involved in its cardioprotective effect observed in obese patients treated with the drug (5). Despite extensive efforts during the last years (6), the exact molecular mechanism (s) of action of metformin still remains incompletely understood, especially the one by which the drug exerts its lipid-lowering action. In 2001, Zhou et al. (7) were the first to report that metformin activates hepatic AMPactivated protein kinase (AMPK), emphasizing the putative role of this energy-sensing kinase in the mechanism of action of the drug.

AMPK is a well-conserved serine/threonine protein kinase that plays a crucial role in the regulation of catabolic/anabolic pathways by acting as a cellular energy and nutrient sensor (8,9). AMPK consists of a heterotrimeric complex containing a catalytic a subunit and two regulatory ß and γ subunits. Each subunit has several isoforms (α1, α2; ß1, ß2; γ1, γ2, γ3) that are encoded by distinct genes, giving multiple heterotrimeric combinations with tissue-specific distribution (8,9). The ß subunit contains a threonine residue (Thr 172) whose phosphorylation by upstream kinases, such as the liver kinase B (LKB1), is required for AMPK activation. The b subunit acts as a scaffold to which the two other subunits are bound and also allows AMPK to sense energy reserves in the form of glycogen (8,9). Binding of AMP and/or ADP to selective domains on the γ subunit leads to AMPK activation via a complex mechanism involving direct allosteric activation, phosphorylation on Thr172 by AMPK upstream kinases, and inhibition of dephosphorylation of this residue by specific protein phosphatases that remain to be identified (8,9). Interestingly, the mechanism by which metformin activates AMPK, involving specific inhibition of the mitochondrial respiratory chain complex 1 (10,11), was recently clarified (12,13), although the contribution of the LKB1/AMPK axis in its hepatic effects still remains controversial (14–18).

The objective of this study was to investigate the molecular mechanisms underlying the effects of metformin on lipoprotein metabolism by using APOE*3-Leiden. CETP (E3L.CETP) transgenic mice, a well-established model of human-like lipoprotein metabolism (19) that also responds to lipid-lowering pharmacological interventions (20–23). Collectively, our data show that treatment of E3L.CETP mice with metformin is able to recapitulate the lipid-lowering effect of the drug evidenced in humans, i.e., causing a reduction in plasma VLDL-TG associated with a parallel mild increase in HDL cholesterol. Remarkably, this effect is not mediated by apparent changes in hepatic VLDL-TG production but rather by a selective increase in VLDL-TG clearance by the brown adipose tissue (BAT). At the molecular level, we found an increase in AMPKα1 activity and protein expression of both hormone-sensitive

lipase (HSL) and mitochondrial respiratory chain complexes, suggesting that metformin, on top of increasing VLDL-TG uptake, also promotes intracellular TG lipolysis and subsequent mitochondrial fatty acid (FA) oxidation in BAT.

RESEARCH DESIGN AND METHODS

Materials
All chemicals were purchased from Sigma-Aldrich (St. Louis, MO).

Ethics
All mouse experiments were performed in accordance with the Institute for Laboratory Animal Research Guide for the Care and Use of Laboratory Animals and have received approval from the university ethical review boards (Leiden University Medical Center).

Animals, Diet, and Metformin Treatment
Homozygous human CETP transgenic mice were crossbred with hemizygous APOE*3-Leiden (E3L) mice at our Institutional Animal Facility to obtain E3L.CETP mice, as previously described (19). In this study, 12-week-old E3L. CETP female mice, housed under standard conditions in conventional cages with ad libitum access to food and water, were fed a Western-type diet containing 0.1% (weight for weight [w/w]) cholesterol (Hope Farms, Woerden, the Netherlands) for 4 weeks. Upon randomization according to body weight, plasma total cholesterol (TC), and TG levels, mice next received Western-type diet with or without 200 mg/kg body weight/day (0.2%, w/w) metformin for 4 weeks. Unless otherwise mentioned, experiments were performed after 4 h of fasting at 1:00 P.M. with food withdrawn at 9:00 A.M.

Plasma Lipid and Lipoprotein Analysis
Plasma was obtained via tail vein bleeding and assayed for TC, TG, and phospholipid (PL) using the commercially available enzymatic kits 236691, 11488872, and 1001140 (Roche Molecular Biochemicals, Indianapolis, IN), respectively. Free FAs were measured using the NEFA-C kit from Wako Diagnostics (Instruchemie, Delfzijl, the Netherlands). The distribution of lipids over plasma lipoprotein fractions was determined using fast protein liquid chromatography. Plasma was pooled per group, and 50 µL of each pool was injected onto a Superose 6 PC 3.2/30 column (Akta System, Amersham Pharmacia Biotech, Piscataway, NJ) and eluted at a constant flow rate of 50 µL/min in 1 mmol/L EDTA in PBS, pH 7.4. Fractions of 50 µL were collected and assayed for TC and TG as described above.

Hepatic VLDL-TG and VLDL-apoB Production
Mice were fasted for 4 h prior to the start of the experiment. During the experiment, mice were sedated with 6.25 mg/kg acepromazine (Alfasan, Woerden, the Netherlands), 6.25 mg/kg

midazolam (Roche, Mijdrecht, the Netherlands), and 0.31 mg/kg fentanyl (Janssen-Cilag, Tilburg, the Netherlands). At t = 0 min, blood was taken via tail bleeding and mice were intravenously injected with 100 µL PBS containing 100 µCi Trans^{35}S label (ICM Biomedicals, Irvine, CA) to measure de novo total apolipoprotein B (apoB) synthesis. After 30 min, the animals received 500 mg tyloxapol (Triton WR-1339; Sigma- Aldrich) per kilogram body weight as a 10% (w/w) solution in sterile saline, to prevent systemic lipolysis of newly secreted hepatic VLDL-TG. Additional blood samples were taken at t = 15, 30, 60, and 90 min after tyloxapol injection and used for determination of plasma TG concentration. After 90 min, the animals were killed and blood was collected by orbital bleeding for isolation of VLDL by density-gradient ultracentrifugation, as previously described (19–23). ^{35}S-apoB was measured in the VLDL fraction, and VLDL-apoB production rate was calculated as dpm.h-1, as previously reported (19–23).

In Vivo Clearance of VLDL-Like Emulsion Particles

Mice were fasted overnight with food withdrawn at 6:00 P.M. During the experiment, mice were sedated as described above. At t = 0 min, blood was taken via tail bleeding and mice received a continuous intravenous infusion of glycerol tri[^{3}H]oleate-labeled emulsion particles mixed with albumin-bound [^{14}C]oleic acid (4.4 µCi [^{3}H]TG and 1.2 µCi [^{14}C]FA; both from GE Healthcare Life Sciences, Little Chalfont, U.K.) at a rate of 100 µL/h for 2.5 h, as previously described (24,25). Blood samples were taken using chilled paraoxoncoated capillaries by tail bleeding at 90 and 120 min of infusion to ensure that steady-state conditions had been reached. Subsequently, mice were killed and organs were quickly harvested and snap frozen in liquid nitrogen. Retention of radioactivity in the saponified tissues was measured per milligram of tissue and corrected for the corresponding plasma-specific activities of [^{3}H]FA and [^{14}C]FA, as previously described (24).

Hepatic Lipid Composition

Liver lipids were extracted as previously described (20). In brief, small liver pieces were homogenized in ice-cold methanol. After centrifugation, lipids were extracted by addition of 1,800 µL CH_3OH:$CHCl_3$ (1:3 volume for volume [v/v]) to 45 µL homogenate, followed by vigorous vortexing and phase separation by centrifugation (14,000 rpm; 15 min at room temperature). The organic phase was dried and dissolved in 2% Triton X-100 in water. TG, TC, and PL concentrations were measured using commercial kits as described above. Liver lipids were expressed as nanomoles per milligram protein, which was determined using the BCA protein assay kit (Pierce, Rockford, IL).

Histology

Interscapular BAT was removed and fixed directly in 4% paraformaldehyde, dehydrated, and embedded in paraffin. Hematoxylin and eosin staining was performed using standard protocols. The area of intracellular lipid vacuoles in BAT was quantified using Image J (NIH).

Cell Culture and Brown Adipocyte Differentiation

T37i cells were cultured and differentiated as described previously (26). Cells were next treated with metformin or vehicle (PBS) for 8 h. Then, supernatant was collected for determination of glycerol (Instruchemie, Delfzijl, the Netherlands) and cells were harvested in ice-cold lysis buffer, as described below.

Western Blot Analysis

Snap-frozen liver and BAT samples (~50 mg) or T37i cells were lysed in ice-cold buffer containing the following: 50 mmol/L HEPES (pH 7.6), 50 mmol/L NaF, 50 mmol/L KCl, 5 mmol/L NaPPi, 1 mmol/L EDTA, 1 mmol/L EGTA, 1 mmol/L dithiothreitol, 5 mmol/L ß-glycerophosphate, 1 mmol/L sodium vanadate, 1% NP40, and protease inhibitor cocktail (Complete; Roche). Western blots were performed as previously described (13). All the primary antibodies used are listed in **SUPPLEMENTARY TABLE 1**. Bands were visualized by enhanced chemiluminescence and quantified using Image J (NIH).

AMPK Assay

AMPK activity was assayed after immunoprecipitation with specific antibodies directed against α1- or α2-AMPK catalytic subunits (Kinasource, Dundee, Scotland), as previously described (14).

RNA/DNA Purification and qRT-PCR

RNA was extracted from snap-frozen liver or BAT samples (~25 mg) using Tripure RNA Isolation Reagent (Roche). Total RNA (1–2 µg) was reverse transcribed, and quantitative real-time PCR was then performed with SYBR Green Core Kit on a MyIQ thermal cycler (Bio-Rad). mRNA expression was normalized to CypD mRNA content and expressed as fold change compared with control mice using the ΔΔCT method. Genomic DNA was extracted using the Qiagen Tissue and Blood Kit (Qiagen, Hilden, Germany). For mitochondrial DNA copy number, ND1 (mitochondrial) and LPL (nuclear) copy numbers were quantified by qRT-PCR. All the primer sequences are listed in **SUPPLEMENTARY TABLE 1**.

Statistical Analysis

All data are expressed as mean ± SEM. Statistical analysis was performed using SPSS 17.0 software package for Windows (SPSS, Chicago, IL) with two-tailed unpaired Student *t* test. Differences between groups were considered statistically significant at $P < 0.05$.

RESULTS

Metformin Reduces Plasma Cholesterol and TG Levels

To investigate the effect of metformin on lipoprotein metabolism, E3L.CETP mice were first fed a cholesterolrich (0.1%) Western-type diet for 4 weeks and next treated with or without

metformin (200 mg/kg body weight/day) added to the diet for another 4 weeks. As compared with the control group, metformin did not affect body weight and composition, food intake and plasma glucose, and insulin and FA levels throughout the intervention period **(SUPPLEMENTARY FIGURE 1)**. However, metformin rapidly reduced both plasma TC (227 and 236% at weeks 2 and 4, respectively; $P < 0.05$) and TGs (226 and 238% at weeks 2 and 4, respectively; $P < 0.05$) in a time-dependent manner **(FIGURES 1A** and **C)**. Plasma lipoprotein profile analysis showed that this lipidlowering effect mostly resulted from a reduction of VLDL particles. In addition, a slight shift in plasma cholesterol profile, from VLDL-C to HDL-C (237 and +37%, respectively), was evidenced **(FIGURES 1B** and **D)**.

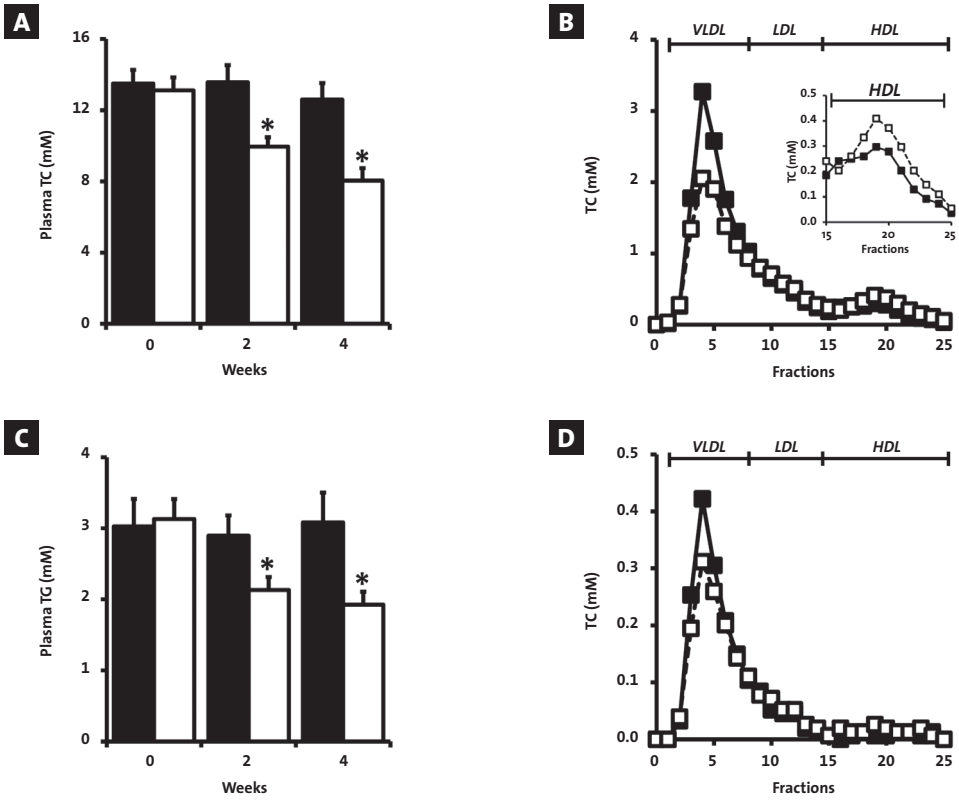

FIGURE 1 - Effect of metformin on plasma cholesterol and TG levels and lipoprotein distribution. Blood samples from 4 h–fasted control (black bars) and metformin-treated (open bars) mice were collected by tail bleeding using chilled paraoxon-coated capillaries at different time points. Plasma TC **A** and TGs **C** levels were determined. The plasma samples collected after 4 weeks of treatment were pooled groupwise and size fractionated by fast protein liquid chromatography. The individual fractions were analyzed for cholesterol **B** and TGs **D**. Data are means ± SEM ($n = 9$ per group).

*$P < 0.05$ vs. control.

Metformin Does Not Affect Hepatic VLDL-TG Production

Plasma VLDL-TG levels are determined by the balance between VLDL-TG production by the liver and VLDL-TG clearance by peripheral organs. Therefore, we first assessed the effect of metformin on hepatic VLDL-TG and -apoB production by injecting Trans^{35}S and tyloxapol in 4 h–fasted control and metformin-treated E3L.CETP mice. Despite the significantly lower basal plasma TG levels (1.72 ± 0.26 vs. 2.65 ± 0.36 mmol/L, $P < 0.05$; data not shown), metformin did not affect the time-dependent accumulation of plasma TG after tyloxapol injection when compared with control E3L.CETP mice **(FIGURE 2A)**. Therefore, the VLDL-TG production

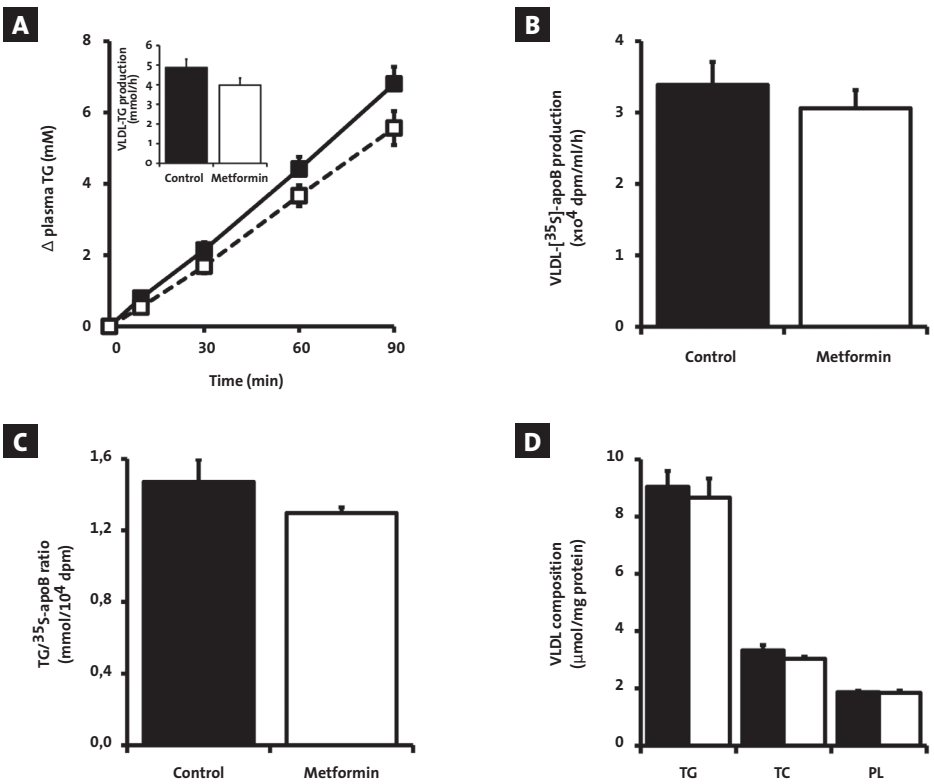

FIGURE 2 - Effect of metformin on hepatic VLDL-TG production. After 4 weeks of treatment, 4 h–fasted control (black squares/bars) and metformin-treated mice (open squares/bars) were injected with Trans^{35}S label ($t = -30$ min) and tyloxapol ($t = 0$ min), and blood samples were drawn up to 90 min after tyloxapol injection. Plasma TG concentrations were determined and plotted as the increase in plasma TG as compared with baseline **A**. The rate of TG production was calculated from the slopes of the curves from the individual mice (**A**, *inset)*. After 120 min, mice were exsanguinated and the total VLDL fraction was isolated by ultracentrifugation. The rate of newly synthesized VLDL-^{35}S-apoB **B**, the TG-to–^{35}S-apoB ratio **C**, as well as the amount of TGs, TC, and PLs per mg VLDL protein **D** were measured. Data are means ± SEM ($n = 5$–8 per group).

*$P < 0.05$ vs. control.

rate, calculated from the slope of the curve, was not significantly different **(FIGURE 2A,** inserted panel), although a trend for a slight decrease can eventually be suggested. The rate of VLDL-apoB production **(FIGURE 2B)**, the ratio of TG-apoB **(FIGURE 2C)**, as well as the composition of the VLDL particles secreted **(FIGURE 2D)** were not significantly altered, indicating that metformin did not affect the hepatic lipidation of VLDL particles. In line with these results, the TG, TC, and PL content in the liver from E3L.CETP mice did not significantly differ between the control and metformin groups, although hepatic TC content tended to be decreased in the metformin-treated group (221%, $P = 0.07$) **(SUPPLEMENTARY FIGURE 2)**. Furthermore, in our experimental conditions, metformin treatment did not affect hepatic AMPK activity, as

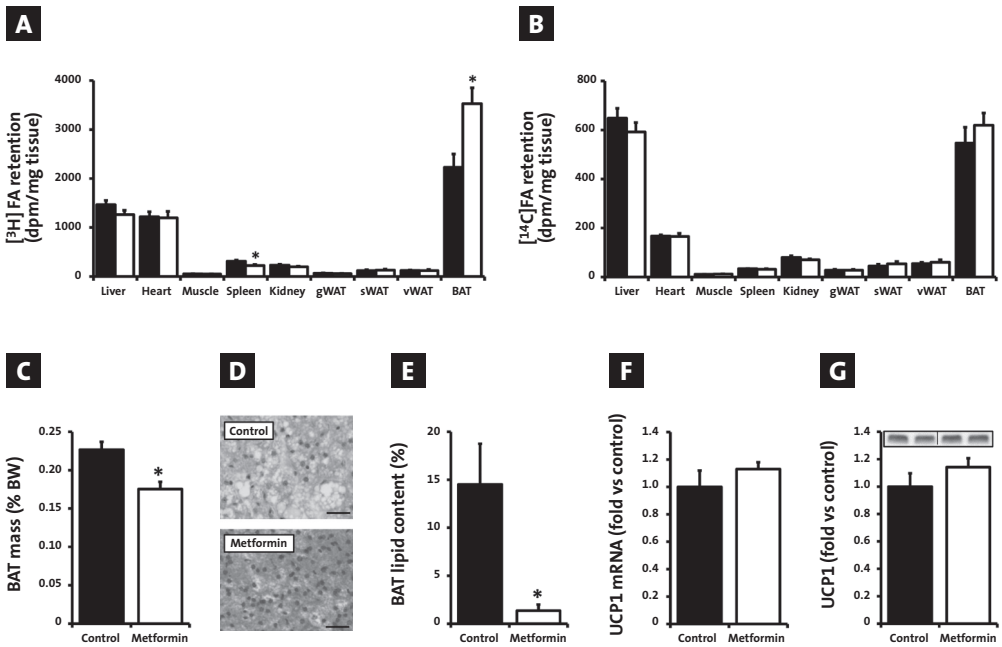

FIGURE 3 - Effect of metformin on peripheral VLDL-TG clearance and BAT. Four hour–fasted control (black bars) and metformin-treated (open bars) mice were continuously infused with [^{3}H]TG-labeled VLDL-like emulsion particles mixed with albumin-bound [^{14}C]FA for 2.5 h. Blood samples were taken using chilled paraoxon-coated capillaries by tail bleeding at 90 and 120 min of infusion to ensure that steadystate conditions had been reached. Subsequently, mice were killed and organs were quickly harvested and snap frozen in liquid nitrogen. Plasma levels of TGs and FAs were determined in plasma, and uptake of the radioactively [^{3}H]TG-labeled emulsion particles **A** and albumin-bound [^{14}C]FA **B** was determined in the organs. In separate experiments, BAT from control and metformin-treated mice were collected and weighed **C**. Hematoxylin and eosin staining of BAT sections was performed, and representative pictures are shown **D**. Relative content of lipid vacuoles in BAT tissue sections ($n = 3–4$ per group) were quantified **E**. mRNA **F** and protein **G** expression of UCP1 were determined by qRT-PCR and Western blot, respectively. Data are means ± SEM ($n = 7–8$ per group).

*$P < 0.05$ vs. control. BW, body weight. (A high-quality color representation of this figure is available in the online issue.)

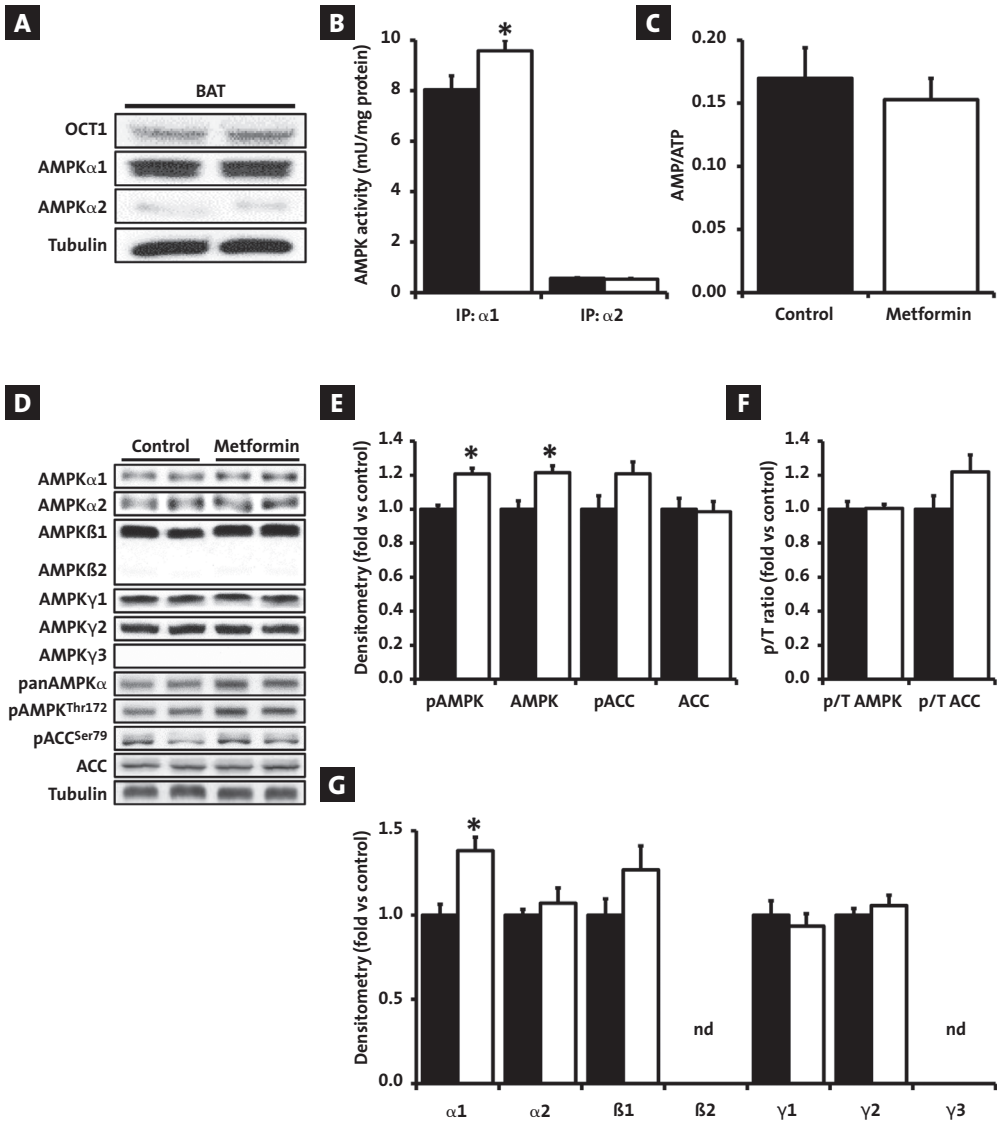

FIGURE 4 - Effect of metformin on AMPK expression, activity, and downstream signaling in BAT. BAT from 4 h–fasted mice was collected after 4 weeks of treatment with (open bars) or without metformin (control, black bars) and immediately snap frozen in liquid nitrogen. The protein expression of OCT1, AMPKα1, and AMPKα2 was determined by Western blot in BAT from control mice **A**. AMPK activity was measured by kinase assay after immunoprecipitation of either AMPKα1 or -α2 catalytic subunits with specific antibodies **B**. Adenine nucleotide concentrations in BAT were measured by high-performance liquid chromatography, and the AMP-to-ATP ratio was calculated **C**. The protein expression of BAT AMPK catalytic (α) and regulatory (ß and γ) subunits, ACC, and the phosphorylation states of Thr172- AMPK and Ser79-ACC were assessed by Western blot **D**, followed by densitometric quantification **E-G**. Tubulin expression was used as internal housekeeping protein. Data are means ± SEM (*n* = 8 per group).

*P < 0.05 vs. control. ND, not detectable.

assessed by phosphorylation of Thr172-AMPK and Ser79-acetyl-CoA carboxylase (ACC), the main downstream target of AMPK **(SUPPLEMENTARY FIGURE 2)**. Finally, we found that hepatic expression of key genes involved in FA/TG uptake, synthesis, and oxidation were not affected, whereas *Lrp1* and *Scarp1,* both involved in cholesterol uptake, were significantly downregulated by metformin **(SUPPLEMENTARY TABLE 1)**. In addition, the expression of *Abca1, Lcat,* and *Pltp* was also found to be significantly downregulated by metformin, suggesting that part of the HDL-enhancing effect of the drug could result from subtle changes in hepatic lipoprotein metabolism.

Metformin Promotes VLDL-TG Clearance by BAT and Influences BAT Mass and Composition

As clearance of TG from plasma is the other major determinant of TG metabolism, the effect of metformin on whole-body lipid partitioning was investigated next. For this purpose, the tissue-specific retention of FA derived from both [^{3}H]TG-labeled VLDL-like emulsion particles and albumin-bound [^{14}C]FA was determined after continuous tracer infusion for 2.5 h. Strikingly, metformin did not affect the uptake of [^{3}H]TG-derived FA by liver, heart, skeletal

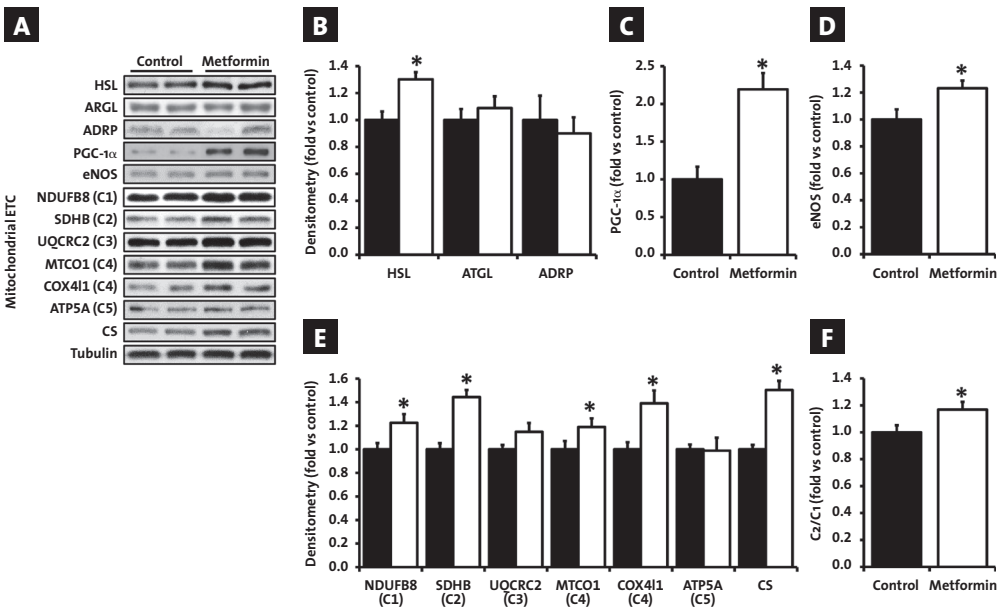

FIGURE 5 - Effect of metformin on expression of key lipolytic and mitochondrial proteins in BAT. BAT was collected in control (black bars) and metformin-treated (open bars) mice, as described in **FIGURE 4**. The protein expression of HSL, ATGL, ADRP, eNOS, PGC-1α, and CS and of various mitochondrial respiratory chain subunits (C1, NDUFB8; C2, SDHB; C3, UQCRC2; C4, MTCO1 and COX4I1; C5, ATP5A) was assessed by Western blot **A**, followed by densitometric quantification **B-E**. Tubulin expression was used as internal housekeeping protein. The ratio of mitochondrial respiratory chain complex 2 to complex 1 was calculated **F**. Data are means ± SEM (n = 8 per group).

*P < 0.05 vs. control. ETC, electron transport chain.

muscle, and various WAT depots but markedly increased ^{3}H retention in BAT (+58%, $P < 0.05$) **(FIGURE 3A)**. The uptake of albumin-bound [^{14}C]FA was not different for any of the organs studied **(FIGURE 3B)**, suggesting that metformin does not affect FA uptake per se but rather promotes lipoprotein lipase (LPL)–mediated VLDL-TG hydrolysis in BAT. Interestingly, BAT mass (–29%) and intracellular lipid droplet content (–91%) were found to be reduced in metformin-treated mice **(FIGURES 3C–E)**, both pointing toward more active BAT (27). However, neither UCP1 mRNA expression nor protein content was significantly affected **(FIGURES 3F** and **G)**.

Metformin Increases AMPK Activity, Lipolytic Machinery, and Mitochondrial Content in BAT

To further investigate the molecular mechanism by which metformin increased VLDL-TG clearance by BAT, we first showed that the organic cation transporter 1 (OCT1), which is crucial for intracellular transport of metformin (28), was expressed in BAT at both transcript (data not shown) and protein levels **(FIGURE 4A)**. We next determined the mRNA expression of genes involved in FA/lipoprotein uptake, FA metabolism, mitochondrial functions, and BAT differentiation but did not find any significant effect of metformin treatment in our

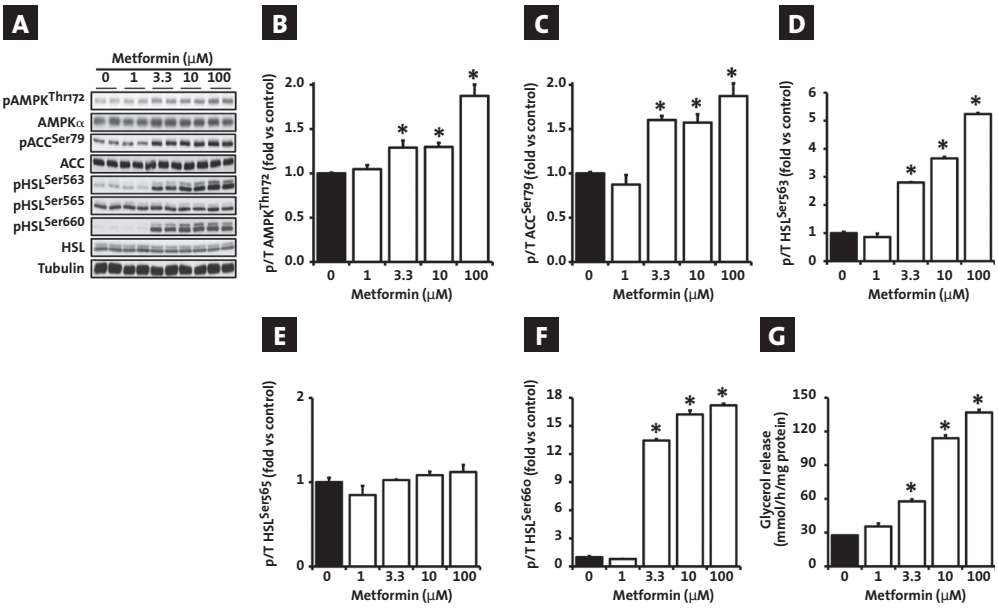

FIGURE 6 - Effect of metformin on AMPK signaling and lipolysis in T37i brown adipocytes. T37i cells were cultured and differentiated in brown adipocytes as described in RESEARCH DESIGN AND METHODS and next treated with increasing concentrations of metformin for 8 h. The protein expression and phosphorylation states of AMPKα, ACC, and HSL on various residues were assessed by Western blot **A** and the phospho-to-total ratios were calculated after densitometric quantification **B-F**. Tubulin expression was used as internal housekeeping protein. The lipolysis rate was assessed by measuring the time-dependent accumulation of glycerol in the culture medium **G** and expressed as μmol/h/mg protein. Data are means ± SEM *(n* = 3).

*$P < 0.05$ vs. control.

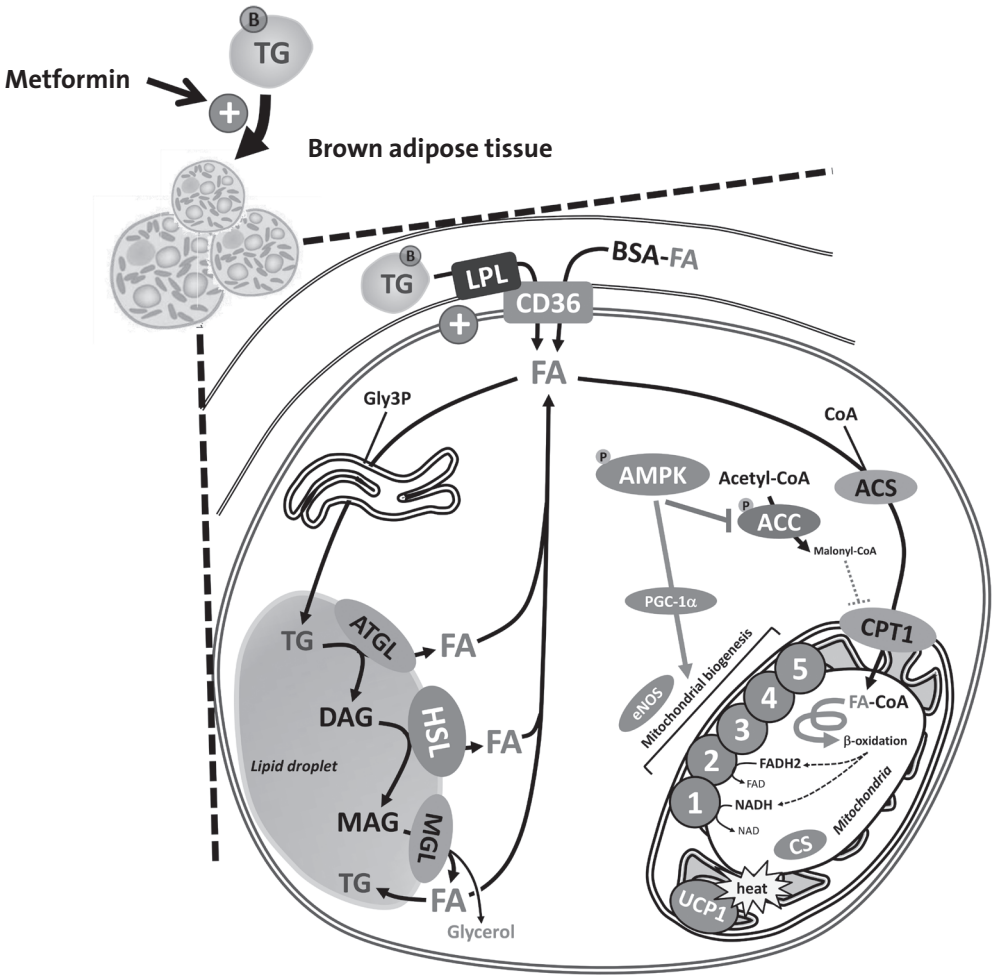

FIGURE 7 - Proposed mechanism for the BAT-mediated TG-lowering effect of metformin. Metformin exerts a beneficial effect on circulating lipids by lowering plasma TG, through a selective increase in TG-derived FA uptake by BAT. In addition, metformin also improves intracellular lipolytic capacity by increasing HSL expression and activity, thereby enhancing FA release from TG stored in lipid droplets. We propose that metformin next promotes FA oxidation in BAT by multiple (path)ways. First, metformin activates AMPK, leading to the subsequent phosphorylation and inactivation of its downstream target ACC. This relieves the inhibition exerted by malonyl-CoA on CPT1, ultimately promoting mitochondrial FA transport and oxidation. Second, metformin increases the tissue mitochondrial content, an effect that might be due to AMPK-mediated stimulation of mitochondrial biogenesis, as reflected by higher expression of eNOS and PGC-1α. Finally, by changing the qualitative composition of the mitochondrial respiratory chain, metformin can enhance respiratory chain complex 2–mediated FA oxidation and UCP1-independent metabolic uncoupling of oxidative phosphorylation.

experimental condition **(SUPPLEMENTARY TABLE 1)**. We confirmed that BAT mostly expressed AMPKα1 **(FIGURE 4A)**, as previously reported (29,30). Interestingly, we found that metformin selectively increased the activity of α1- (+19%, $P < 0.05$) but not of α2-containing AMPK heterotrimers in BAT **(FIGURE 4B)** without affecting the whole-tissue energy state, as assessed by the AMP-ATP ratio **(FIGURE 4C)**. This was associated with a significant increase in both Thr172 phosphorylation (+21%, $P < 0.05$) and expression of the AMPKα catalytic subunits (+21%, $P < 0.05$), whereas the phospho-to-total ratio was not affected **(FIGURES 4D–F)**. However, a trend for increased phosphorylation of the AMPK downstream target ACC was evidenced (+22%, $P = 0.07$) **(FIGURES 4D–F)**. The only AMPK subunit significantly increased by metformin was the α1 isoform (+38%, $P < 0.05$), whereas the other subunits were not affected **(FIGURE 4G)**, suggesting that the higher AMPK activity in BAT from metformin-treated mice was mostly due to an increase in AMPKα1 content. We next examined whether some of the key players involved in the regulation of TG lipolysis and FA oxidation in BAT were affected by metformin. Interestingly, the protein expression of the lipolytic enzyme HSL, but not that of adipose TG lipase (ATGL) and adipose differentiation– related protein (ADRP), was significantly increased by metformin in BAT (+30%, $P < 0.05$) **(FIGURES 5A** and **B)**. In addition, although the mitochondrial DNA content was not affected (data not shown), we found a marked increase in protein expression of two of the main regulators of mitochondrial biogenesis, endothelial nitric oxide synthase (eNOS) and PGC-1α (+23 and +127%, respectively; $P < 0.05$), together with a significantly higher content of citrate synthase (CS) and of most of the mitochondrial electron transport chain complexes in BAT from metformin-treated E3L.CETP mice **(FIGURES 5A** and **C–E)**. Of note, the ratio of mitochondrial respiratory chain complex 2 to complex 1 expression was also increased by metformin in BAT (+17%, $P < 0.05$) **(FIGURE 5F)**.

Metformin Induces AMPK Activation and Lipolysis in T37i Brown Adipocytes

To investigate whether metformin can directly affect AMPK activity and lipid metabolism in BAT, we used T37i cells, a well-established in vitro model of differentiated brown adipocytes (26). Interestingly, we showed that therapeutic concentrations of metformin dose-dependently increased phosphorylation states of AMPK, ACC, and HSL **(FIGURES 6A–F)**, as well as glycerol release into the medium, pointing toward enhanced intracellular lipolysis **(FIGURE 6G)**. Taken together, our results show that metformin not only promotes VLDL-TG uptake by BAT but also enhances both intracellular lipolytic and mitochondrial FA ß-oxidation capacity in this tissue **(FIGURE 7)**.

DISCUSSION

Metformin not only improves glycemic control in type 2 diabetic patients but also exerts beneficial effects on plasma lipid profiles (4) by a mechanism that has remained, so far, poorly understood. In the current study, we have therefore investigated the molecular mechanism(s) underlying this lipid-lowering property of metformin using E3L.CETP mice, a

well-characterized transgenic model displaying a human-like lipoprotein metabolism and human-like responses to lipid-modulating drugs when fed a Western-type diet (19–23). Our results show that chronic treatment of E3L.CETP mice with metformin recapitulates the effects on circulating lipoproteins observed in patients treated with the drug, i.e., reduction in plasma TG associated with significant reduction in VLDL (31). We next demonstrated that metformin does not affect hepatic VLDL-TG production but instead selectively promotes VLDL-TG clearance by BAT, an effect associated with elevated components of intracellular lipolytic and mitochondrial FA oxidation machinery in this highly active metabolic tissue. To the best of our knowledge, this study is the first one reporting that BAT is involved in the lipid-lowering effect of metformin, and therefore constitutes an important target tissue for the drug.

Plasma TG levels are determined by the balance between production of chylomicron-TG and VLDL-TG in intestine and liver, respectively, and their LPL-mediated TG clearance in peripheral tissues. In our study, all the experiments were performed in fasted mice, thereby excluding any significant contribution of intestine-derived chylomicrons to the change observed in circulating TG concentrations. Furthermore, metformin treatment did not affect the postprandial response to an oral lipid load **(SUPPLEMENTARY FIGURE 3)**, suggesting that impaired intestinal TG absorption is not involved in the TG-lowering effect of the drug. Besides its central role in glucose homeostasis, the liver plays a key role in lipid metabolism, notably by regulating synthesis and secretion of apoB-containing VLDL-TG particles (32). Hepatic VLDLTG production is mostly driven by intracellular substrate availability resulting from both FA uptake from the circulation and the balance between de novo lipogenesis and mitochondrial FA ß-oxidation in the liver (33). In our study, we found that metformin did not significantly affect plasma FA levels; hepatic lipid content; AMPK activity; expression of genes involved in FA/TG uptake, synthesis, and oxidation; VLDL-TG and VLDL-apoB secretion rates; and composition of the excreted VLDL particles. Although we did not find an apparent contribution of the liver to the TG-reducing effect of metformin, we cannot completely exclude that some of its hepatic effects were lowered or masked due to our experimental conditions, e.g., fasting state, and the pharmacokinetic features of the drug. Of note, we found that expression of some genes involved in hepatic HDL uptake *(Lrp1* and *Scarb1)* and remodeling *(Abca1* and *Pltp)* was decreased by metformin, suggesting that part of the mild HDL-raising effect of the drug might be partly due to subtle changes in cholesterol metabolism in the liver. Future studies are required for clarifying the exact underlying molecular mechanism.

Plasma VLDL-TG clearance is driven by LPL-mediated lipolysis in the capillaries of peripheral tissues (34). The most striking result of our present study was that metformin induced a potent and selective increase in VLDLglycerol tri[^{3}H]oleate-derived [^{3}H]oleate retention in BAT without affecting VLDL-TG uptake by heart, muscle, and various white adipose tissues. Recently, Bartelt et al. (35) were the first to identify BAT as a major organ involved in plasma VLDL-TG clearance in rodents. In this elegant study confirming previous observations (36), they reported that BAT constitutes a quantitatively relevant lipid-clearing organ displaying very high rates of VLDL-TG uptake (35) by a mechanism that still remains to be fully charac-

terized. In the current study, our observation that metformin promotes VLDL-[^{3}H]TG–derived FA but not albumin-bound [^{14}C]FA retention in BAT suggests that the TG-lowering effect of the drug is mediated by a tissue-specific increase in LPL-mediated VLDL-TG hydrolysis with subsequent retention of the liberated FA in BAT. At the molecular level, it remains to be clarified whether increases in endothelial LPL expression and/or subtle changes in apolipoproteins and angiopoietin-like proteins regulating local LPL activity (37) are involved in the BAT-specific VLDL-derived TG hydrolysis induced by metformin.

Owing to its high mitochondrial and oxidative enzyme content, BAT has a marked ability to oxidize both glucose and FA, the latter being derived from either LPL-mediated hydrolysis of VLDL-TG or intracellular TG that is stored in lipid droplets. Once released, FAs are rapidly reesterified in TG or directed to mitochondria for oxidation or activation of UCP1, leading to dissipation of the proton gradient across the inner mitochondrial membrane and heat production (38). At the molecular level, we found that metformin, both in vivo and in vitro, increased AMPK activity and Ser79-ACC phosphorylation, an effect that is expected to promote mitochondrial FA transport and oxidation by relieving the inhibition of CPT1α by malonyl-CoA (9). AMPK activation is known to trigger mitochondrial biogenesis, at least in skeletal muscle (39) and liver (40). Interestingly, the expression of key proteins of the mitochondrial respiratory chain complexes and CS was increased by metformin in BAT, indicating enhanced mitochondrial content in this tissue. Mechanistically, the expression of PGC-1α and eNOS, which are both recognized as important regulators of mitochondrial biogenesis (41,42), were found to be higher in BAT from metformin-treated mice, suggesting activation of the AMPK-PGC1α-eNOS pathway by metformin in this tissue. Finally, we found that metformin affected the qualitative composition of the mitochondrial respiratory chain in BAT, leading to an increase in complex 2 relative to complex 1. This effect might also contribute to enhanced FA oxidation by promoting electron supply to the respiratory chain complex 2. Interestingly, modulating the ratio of $FADH_2$ to NADH oxidation will also affect the stoichiometry of oxidative phosphorylation and promote UCP1-independent metabolic uncoupling, with the yield of ATP synthesis being lowered by ~40% when $FADH_2$ is oxidized as compared with NADH (43). Taken together, we propose that secondary to its tissue-specific increase in VLDL-TG uptake, metformin promotes FA oxidation in BAT by enhancing both intracellular lipolytic capacity and mitochondrial oxidative machinery. It is important to underline that we do not exclude that another AMPKindependent mechanism(s) in BAT might also contribute to the TG-lowering effect of metformin in vivo.

The recent discovery of metabolically active BAT in adult humans (44–46) has caused a revival interest in this potential new therapeutic target for the treatment of obesity and metabolic disorders (47,48). Although the precise role of BAT in TG metabolism remains to be established, it has been recently shown that FA uptake and oxidation in BAT significantly contributes to energy expenditure in humans (49). Thus, it is tempting to speculate that part of the weight-lowering property of metformin might be secondary to enhanced lipid oxidation and energy dissipation in BAT. Further studies allowing imaging of lipid metabolism in BAT from metformin- treated patients, for instance using ^{18}F-labeled FA incorporated into VLDL-TG coupled to position emission tomography scanning (50), would be crucial to

specifically address this point.

In summary, we show that metformin exerts a beneficial effect on circulating lipids by lowering plasma TG, through a selective BAT-mediated increase in VLDL-TG uptake/lipolysis **(FIGURE 7)**. The current study is the first identifying BAT as a new important mechanistic player in the lipid-lowering action of metformin, suggesting that targeting this tissue, on top of being interesting for body weight management, might also be of therapeutic importance in the treatment of dyslipidemia.

ACKNOWLEDGMENTS

The authors are grateful to Elsbet Pieterman, Chris van der Bent, Linda Switzar, and Amanda Pronk (Leiden University Medical Center) for their valuable technical assistance.

REFERENCES

1 Goodarzi MO, Bryer-Ash M. Metformin revisited: re-evaluation of its properties and role in the pharmacopoeia of modern antidiabetic agents. Diabetes Obes Metab 2005;7:654–665.

2 Nathan DM, Buse JB, Davidson MB, et al.; American Diabetes Association; European Association for the Study of Diabetes. Medical management of hyperglycaemia in type 2 diabetes mellitus: a consensus algorithm for the initiation and adjustment of therapy: a consensus statement from the American Diabetes Association and the European Association for the Study of Diabetes. Diabetologia 2009;52:17–30.

3 Natali A, Ferrannini E. Effects of metformin and thiazolidinediones on suppression of hepatic glucose production and stimulation of glucose uptake in type 2 diabetes: a systematic review. Diabetologia 2006;49:434–441.

4 Salpeter SR, Buckley NS, Kahn JA, Salpeter EE. Meta-analysis: metformin treatment in persons at risk for diabetes mellitus. Am J Med 2008;121: 149–157.e2.

5 UK Prospective Diabetes Study (UKPDS) Group. Effect of intensive bloodglucose control with metformin on complications in overweight patients with type 2 diabetes (UKPDS 34). Lancet 1998a;352:854–865.

6 Viollet B, Guigas B, Sanz Garcia N, Leclerc J, Foretz M, Andreelli F. Cellular and molecular mechanisms of metformin: an overview. Clin Sci (Lond) 2012;122:253–270.

7 Zhou G, Myers R, Li Y, et al. Role of AMP-activated protein kinase in mechanism of metformin action. J Clin Invest 2001; 108:1167–1174.

8 Carling D, Thornton C, Woods A, Sanders MJ. AMP-activated protein kinase: new regulation, new roles? Biochem J 2012;445:11–27.

9 Hardie DG, Ross FA, Hawley SA. AMPK: a nutrient and energy sensor that maintains energy homeostasis. Nat Rev Mol Cell Biol 2012;13:251–262.

10 El-Mir MY, Nogueira V, Fontaine E, Avéret N, Rigoulet M, Leverve X. Dimethylbiguanide inhibits cell respiration via an indirect effect targeted on the respiratory chain complex I. J Biol Chem 2000;275:223–228.

11 Owen MR, Doran E, Halestrap AP. Evidence that metformin exerts its antidiabetic effects through inhibition of complex 1 of the mitochondrial respiratory chain. Biochem J 2000;348:607–614.

12 Hawley SA, Ross FA, Chevtzoff C, et al. Use of cells expressing gamma subunit variants to identify diverse mechanisms of AMPK activation. Cell Metab 2010;11:554–565.

13 Stephenne X, Foretz M, Taleux N, et al. Metformin activates AMP-activated protein kinase in primary human hepatocytes by decreasing cellular energy status. Diabetologia 2011;54:3101–3110.

14 Guigas B, Bertrand L, Taleux N, et al. 5-Aminoimidazole-4-carboxamide-1-beta-D-ribofuranoside and metformin inhibit hepatic glucose phosphorylation by an AMP-activated protein kinase-independent effect on glucokinase translocation. Diabetes 2006;55:865–874.

15 Foretz M, Hébrard S, Leclerc J, et al. Metformin inhibits hepatic gluconeogenesis in mice independently of the LKB1/AMPK pathway via a decrease in hepatic energy state. J Clin Invest 2010;120:2355–2369.

16 Shaw RJ, Lamia KA, Vasquez D, et al. The kinase LKB1 mediates glucose homeostasis in liver and therapeutic effects of metformin. Science 2005; 310:1642–1646.

17 Kalender A, Selvaraj A, Kim SY, et al. Metformin, independent of AMPK, inhibits mTORC1 in a rag GTPase-dependent manner. Cell Metab 2010;11: 390–401.

18 Miller RA, Chu Q, Xie J, Foretz M, Viollet B, Birnbaum MJ. Biguanides suppress hepatic glucagon signalling by decreasing production of cyclic AMP. Nature 2013;494:256–260.

19 Westerterp M, van der Hoogt CC, de Haan W, et al. Cholesteryl ester transfer protein decreases high-density lipoprotein and severely aggravates atherosclerosis in APOE*3-Leiden mice. Arterioscler Thromb Vasc Biol 2006;26:2552–2559.
20 Bijland S, Pieterman EJ, Maas AC, et al. Fenofibrate increases very low density lipoprotein triglyceride production despite reducing plasma triglyceride levels in APOE*3-Leiden.CETP mice. J Biol Chem 2010; 285: 25168–25175.
21 Bijland S, van den Berg SA, Voshol PJ, et al. CETP does not affect triglyceride production or clearance in APOE*3-Leiden mice. J Lipid Res 2010;51:97–102.
22 de Haan W, van der Hoogt CC, Westerterp M, et al. Atorvastatin increases HDL cholesterol by reducing CETP expression in cholesterol-fed APOE*3-Leiden.CETP mice. Atherosclerosis 2008;197:57–63
23 van der Hoorn JW, de Haan W, Berbée JF, et al. Niacin increases HDL by reducing hepatic expression and plasma levels of cholesteryl ester transfer protein in APOE*3Leiden.CETP mice. Arterioscler Thromb Vasc Biol 2008; 28:2016–2022.
24 Coomans CP, Geerling JJ, Guigas B, et al. Circulating insulin stimulates fatty acid retention in white adipose tissue via KATP channel activation in the central nervous system only in insulin-sensitive mice. J Lipid Res 2011;52:1712–1722.
25 Teusink B, Voshol PJ, Dahlmans VE, et al. Contribution of fatty acids released from lipolysis of plasma triglycerides to total plasma fatty acid flux and tissue-specific fatty acid uptake. Diabetes 2003;52:614–620.
26 Zennaro MC, Le Menuet D, Viengchareun S, Walker F, Ricquier D, Lombès M. Hibernoma development in transgenic mice identifies brown adipose tissue as a novel target of aldosterone action. J Clin Invest 1998; 101:1254–1260.
27 Ortega-Molina A, Efeyan A, Lopez-Guadamillas E, et al. Pten positively regulates brown adipose function, energy expenditure, and longevity. Cell Metab 2012;15:382–394.
28 Shu Y, Sheardown SA, Brown C, et al. Effect of genetic variation in the organic cation transporter 1 (OCT1) on metformin action. J Clin Invest 2007;117:1422–1431.
29 Pulinilkunnil T, He H, Kong D, et al. Adrenergic regulation of AMP-activated protein kinase in brown adipose tissue in vivo. J Biol Chem 2011;286: 8798–8809.
30 Mulligan JD, Gonzalez AA, Stewart AM, Carey HV, Saupe KW. Upregulation of AMPK during cold exposure occurs via distinct mechanisms in brown and white adipose tissue of the mouse. J Physiol 2007;580:677–684.
31 Jonker JT, Wang Y, de Haan W, et al. Pioglitazone decreases plasma cholesteryl ester transfer protein mass, associated with a decrease in hepatic triglyceride content, in patients with type 2 diabetes. Diabetes Care 2010; 33:1625–1628.
32 Xiao C, Hsieh J, Adeli K, Lewis GF. Gut-liver interaction in triglyceride-rich lipoprotein metabolism. Am J Physiol Endocrinol Metab 2011;301:E429–E446.
33 Nielsen S, Karpe F. Determinants of VLDL-triglycerides production. Curr Opin Lipidol 2012;23:321–326.
34 Dallinga-Thie GM, Franssen R, Mooij HL, et al. The metabolism of triglyceride-rich lipoproteins revisited: new players, new insight. Atherosclerosis 2010;211:1–8.
35 Bartelt A, Bruns OT, Reimer R, et al. Brown adipose tissue activity controls triglyceride clearance. Nat Med 2011;17:200–205.
36 Hagberg CE, Falkevall A, Wang X, et al. Vascular endothelial growth factor B controls endothelial fatty acid uptake. Nature 2010;464:917–921.
37 Davies BS, Beigneux AP, Fong LG, Young SG. New wrinkles in lipoprotein lipase biology. Curr Opin Lipidol 2012;23:35–42.

38 Festuccia WT, Blanchard PG, Deshaies Y. Control of brown adipose tissue glucose and lipid metabolism by PPARg. Front Endocrinol (Lausanne) 2011;2:84.
39 Zong H, Ren JM, Young LH, et al. AMP kinase is required for mitochondrial biogenesis in skeletal muscle in response to chronic energy deprivation. Proc Natl Acad Sci USA 2002;99:15983–15987.
40 Guigas B, Taleux N, Foretz M, et al. AMP-activated protein kinase-independent inhibition of hepatic mitochondrial oxidative phosphorylation by AICA riboside. Biochem J 2007;404:499–507.
41 Jornayvaz FR, Shulman GI. Regulation of mitochondrial biogenesis. Essays Biochem 2010;47:69–84.
42 Lira VA, Brown DL, Lira AK, et al. Nitric oxide and AMPK cooperatively regulate PGC-1 in skeletal muscle cells. J Physiol 2010;588:3551–3566.
43 Leverve XM, Taleux N, Favier R, et al. Cellular energy metabolism and integrated oxidative phosphorylation. In *Molecular System Bioenergetics: Energy for Life*. Saks V, Ed. Weinheim, WILEY-VCH Verlag GmbH & Co., 2007, p. 11–27.
44 Cypess AM, Lehman S, Williams G, et al. Identification and importance of brown adipose tissue in adult humans. N Engl J Med 2009;360:1509–1517.
45 van Marken Lichtenbelt WD, Vanhommerig JW, Smulders NM, et al. Coldactivated brown adipose tissue in healthy men. N Engl J Med 2009;360: 1500–1508.
46 Virtanen KA, Lidell ME, Orava J, et al. Functional brown adipose tissue in healthy adults. N Engl J Med 2009;360:1518–1525.
47 Ravussin E, Galgani JE. The implication of brown adipose tissue for humans. Annu Rev Nutr 2011;31:33–47.
48 Seale P, Kajimura S, Spiegelman BM. Transcriptional control of brown adipocyte development and physiological function—of mice and men. Genes Dev 2009;23:788–797.
49 Ouellet V, Labbé SM, Blondin DP, et al. Brown adipose tissue oxidative metabolism contributes to energy expenditure during acute cold exposure in humans. J Clin Invest 2012;122:545–552.
50 Labbé SM, Grenier-Larouche T, Croteau E, et al. Organ-specific dietary fatty acid uptake in humans using positron emission tomography coupled to computed tomography. Am J Physiol Endocrinol Metab 2011;300:E445–E453.

SUPPLEMENTARY DATA

SUPPLEMENTARY TABLE 1 - **Primary antibodies for Western blots**

Primary antibody	Residue	Supplier	Reference	Dilution
ACC	-	Cell Signaling	#3662	1:2000
ACC	Ser79	Cell Signaling	#3661	1:2000
ADRP	-	AbCam	Ab108323	1:1000
AMPKα	-	Cell Signaling	#2532	1:1000
AMPKα	Thr172	Cell Signaling	#2535	1:1000
AMPKα1	-	Kinasource	AB-140	1:2500
AMPKα2	-	Kinasource	AB-141	1:2500
ATGL	-	Cell Signaling	#2439	1:1250
ATP5A (C5)	-	AbCam	ab110413	1:1000
COX4I1 (C4)	-	Aviva Systems Biology	ARP42784	1:500
CS	-	AbCam	Ab96600	1:1000
HSL	-	Cell Signaling	#4107	1:2000
HSL	Ser563	Cell Signaling	#4139	1:2000
HSL	Ser565	Cell Signaling	#4137	1:1000
HSL	Ser660	Cell Signaling	#4126	1:1000
MTCO1 (C4)	-	AbCam	ab110413	1:1000
NDUFB8 (C1)	-	AbCam	ab110413	1:1000
eNOS (NOS3)	-	Santa Cruz	sc-654	1:1000
OCT1	-	Santa Cruz	sc-133866	1:500
PGC1α	-	AbCam	ab54481	1:1000
UCP1	-	Sigma	U6382	1:2500
UQCRC2 (C3)	-	AbCam	ab110413	1:1000
SDHB (C2)	-	AbCam	ab110413	1:1000
Tubulin	-	Cell Signaling	#2148	1:2000

SUPPLEMENTARY TABLE 2 - **Primer sequences for qRT-PCR**

Gene	Accession number	Forward primer	Reverse primer
Abca1	NM_013454.3	CCCAGAGCAAAAAGCGACTC	GGTCATCATCACTTTGGTCCTTG
Abcg5	NM_031884	TGTCCTACAGCGTCAGCAACC	GGCCACTCTCGATGTACAAGG
Abcg8	NM_026180	TCCTGTGAGCTGGGCATCCGA	CCCGCAGCCTGAGCTCCCTAT
Acaca	NM_133360.2	CAGCTGGTGCAGAGGTACCG	TCTACTCGCAGGTACTGCCG
Acacb	NM_133904.2	GCGCCTACTATGAGGCCCAGCA	ACAAACTCGGCTGGGGACGC
Acly	NM_134037.2	TGTGGACGGCTTCATCGGCG	ATGTCATCCCAGGGGTGACG
Acox1	NM_015729	GGGACCCACAAGCCTCTGCCA	GTGCCGTCAGGCTTCACCTGG
Apoa1	NM_009692	TGCGGTCAAAGACAGCGGCA	AGATTCAGGTTCAGCTGTTGGCCC
Apob	NM_009693	CAGCTGCAAGTGTCCTCGTC	GACACAGAGGGCTTTGCCAC

Gene	Accession number	Forward primer	Reverse primer
Atp5a1	NM_007505.2	CCAAGCAGGCTGTCGCTTACCG	TCTCCAGCAGGCGGGAGTGT
Cd36	NM_001159558	GCAAAGAACAGCAGCAAAATC	CAGTGAAGGCTCAAAGATGG
Cidea	NM_007702	CTCGGCTGTCTCAATGTCAA	CCGCATAGACCAGGAACTGT
Cidec	NM_178373	CCATCAGAACAGCGCAAGAAG	AGAGGGTTGCCTTCACGTTC
Cox7a1	NM_009944.3	AAAACCGTGTGGCAGAGAAG	CCAGCCCAAGCAGTATAAGC
Cpt1a	NM_013495	AGGAGACAAGAACCCCAACA	AAGGAATGCAGGTCCACATC
Creb1	NM_133828	AGCTGCCACTCAGCCGGGTA	TCGCCTGAGGCAGCTTGAACA
Cs	NM_026444.3	GCTAAGTACTGGGAGCTCATCTAT	GCCTAGAGTCAATGGCTCCG
Dgat1	NM_010046.2	CTAGTGAGCGTTCCCCTGCG	GGGCATCGTAGTTGAGCACG
Dio2	NM_010050	CGCTCCAAGTCCACTCGCGG	CGGCCCCATCAGCGGTCTTC
Fabp1	NM_017399.4	GCCACCATGAACTTCTCCGGCA	GGTCCTCGGGCAGACCTATTGC
Fasn	NM_007988	CACAGGCATCAATGTCAACC	TTTGGGAAGTCCTCAGCAAC
*Fdft*1	NM_010191.2	CCAACTCAATGGGTCTGTTCCT	TGGCTTAGCAAAGTCTTCCAACT
Fdps	NM_134469.4	ATGGAGATGGGCGAGTTCTTC	CCGACCTTTCCCGTCACA
Gpam	NM_008149.3	TCATACCCGTGGGCATCTCG	AATCCACTCGGACGTAGCCG
Gpihbp1	NM_026730	AGTGGACAGCCAGGGAGTGGC	GCTCTCCCCGCTGTGAAGCAC
Hmgcr	NM_008255	CTTGTGGAATGCCTTGTGATTG	AGCCGAAGCAGCACATGAT
Hmgcs1	NM_145942.4	GGACTGGAAGCCTTTGGGGACG	TGCCAGGACAGAAGCCAGGGA
Hmgcs2	NM_008256.4	CATCGCAGGAAGTATGCCCG	GCTGTTTGGGTAGCAGCTCG
Idi1	NM_145360.2	TGGGAATACCCTTGGAAGAGGTTGA	CCCCAGATACCATCAGATTGGGCCT
Lcat	NM_008490.2	GGCAAGACCGAATCTGTTGAG	ACCAGATTCTGCACCAGTGTGT
Ldlr	NM_010700	GCATCAGCTTGGACAAGGTGT	GGGAACAGCCACCATTGTTG
Lipe	NM_010719	AGCCTCATGGACCCTCTTCT	GCCTAGTGCCTTCTGGTCTG
Lpl	NM_008509	CAGGGGGTCACCTGGTCGAAGT	AGCTGGTCCACGTCTCCGAGT
Lrp1	NM_008512	GGAACTCCAGTCGCTGCAAC	TAGCACAGGGATGTCCGCTC
Mttp	NM_008642	GCCTGTGGCTTTGCCACCCA	TCCACCACTGCCTTGAGCTTGC
ND1	NP_904328.1	CTACAACCATTTGCAGACGC	GGAACTCATAGACTTAATGC
Ndufb8	NM_026061.2	GAGGCACGGAGAGCCTTCCA	GGGAGCATCGGGTAGTCGCC
Nr1h3	NM_013839.4	CTGCACGCCTACGTCTCCAT	AAGTACGGAGGCTCACCAGCT
Pltp	NM_011125.2	GGCCGTCTCAGTGCTAAGTT	CGAAGTTGATACCCTCAGGAA
Pnpla2	NM_001163689	TTCGCAATCTCTACCGCCTC	TGGTTCAGTAGGCCATTCCTC
Plin2	NM_007408.3	CAGGATGGAGGAAAGACTGC	CTTATCCACCACCCCTGAGA
Plin4	NM_020568.3	TGCCCCCTCATCTAAAGTGTC	AGGCATCTTCACTGCTGGTC
Plin5	NM_001077348.1	TGTCCAGTGCTTACAACTCGG	CAGGGCACAGGTAGTCACAC
Ppara	NM_011144	CAACCCGCCTTTTGTCATAC	CCTCTGCCTCTTTGTCTTCG
Pparg	NM_011146	CCTGCGGAAGCCCTTTGGTGA	AGCCTGGGCGGTCTCCACTG
Ppargc1a	NM_008904.2	TGCTAGCGGTTCTCACAGAG	AGTGCTAAGACCGCTGCATT
Ppargc1b	NM_133249	CTTGCTTTTCCCAGATGAGG	CCCTGTCCGTGAGGAACG
Prkaa1	NM_001013367	TGGTGGGAAAAATCCGCCGGG	CGGCTTTCCTTTTCGTCCAACCTTC
Prkaa2	NM_178143	ACCGAGCTATGAAGCAGCTGGGTT	CCTCTGCTCCACCACCTCATCATC
Scarb1	NM_016741	TCGCTTCACGGCCCCCGATA	ACAGAGGCGCACCAAACCTGC

Gene	Accession number	Forward primer	Reverse primer
Scd1	NM_009127.4	GCTCTACACCTGCCTCTTCGGGAT	TCCAGAGGCGATGAGCCCCG
Sdha	NM_023281.1	GGGACAGGTGCTGAAGCATGTGAAT	GCAATGCTCAGGGCACAGGCT
Sdhb	NM_023374.3	CGACGGTCGGGGTCTCCTTGA	CCTGAAACTGCAGGCCGACTC
Sqle	NM_009270.3	TCGTTCGTGACGGACCCGGA	ACTGTATCTCCAAGGCCCAGCTCC
Srebf1	NM_011480	GGCCGAGATGTGCGAACT	TTGTTGATGAGCTGGAGCATGT
Srebf1	NM_011480	CTGGCTGAGGCGGGATGA	TACGGGCCACAAGAAGTAGA
Tfam	NM_009360	CTTCCTGGGTTCACCCGCAC	ATGGGCACTATGGCTCCGTC
Ucp1	NM_009463	TCAGGATTGGCCTCTACGAC	TGCATTCTGACCTTCACGAC
Vldlr	NM_013703	TCTTGAGCAGTGTGGCCGTC	TTGCAGTCAGGGTCTCCGTC

SUPPLEMENTARY TABLE 3 - **Effect of metformin on hepatic expression of genes involved in FA/TG and lipoprotein metabolism.** Livers were isolated from 4 h-fasted mice treated with or without metformin for 4 weeks. mRNA expression of the indicated genes were quantified by RT-PCR relative to CypD gene and expressed as fold difference compared with the control group. Data are means ± SEM (n=8). *, p<0.05.

Genes by function	Protein	Fold change	
		Control	Metformin
FA uptake			
Fabp1	**FABP1**	1.00 ± 0.16	1.16 ± 0.14
Cd36	**CD36**	1.00 ± 0.13	0.89 ± 0.06
Lpl	**LPL**	1.00 ± 0.07	0.83 ± 0.10
FA/TG synthesis			
Srebf1	**SREBP-1A**	1.00 ± 0.14	0.84 ± 0.16
Srebf1	**SREBP-1C**	1.00 ± 0.06	0.94 ± 0.09
Nr1h3	**LXRα**	1.00 ± 0.06	0.97 ± 0.04
Fasn	**FAS**	1.00 ± 0.16	0.97 ± 0.25
Scd1	**SCD1**	1.00 ± 0.22	0.82 ± 0.16
Dgat1	**DGAT1**	1.00 ± 0.13	0.89 ± 0.10
FA oxidation			
Pparagc1a	**PGC1α**	1.00 ± 0.10	0.72 ± 0.16
Ppara	**PPARα**	1.00 ± 0.10	0.93 ± 0.06
Cpt1a	**CPT1α**	1.00 ± 0.05	0.94 ± 0.06
Acaca	**ACC1**	1.00 ± 0.12	0.83 ± 0.14
Acacb	**ACC2**	1.00 ± 0.22	1.07 ± 0.13
Acox1	**ACOX1**	1.00 ± 0.06	0.92 ± 0.09
Lipoprotein uptake			
Ldlr	**LDLr**	1.00 ± 0.10	0.96 ± 0.12
Lrp1	**LRP1**	1.00 ± 0.09	**0.85 ± 0.07***
Scarb1	**SRB1**	1.00 ± 0.05	**0.86 ± 0.05***

Genes by function	Protein	Fold change	
		Control	Metformin
VLDL synthesis			
Apob	**ApoB**	1.00 ± 0.05	0.88 ± 0.07
Mttp	**MTP**	1.00 ± 0.10	0.95 ± 0.12
Cholesterol synthesis			
Srbp2	**SRBP2**	1.00 ± 0.06	1.07 ± 0.11
Hmgcr	**HMG CoA-R**	1.00 ± 0.15	1.13 ± 0.21
Hmgcs1	**HMG CoA-S1**	1.00 ± 0.10	1.04 ± 0.18
Hmgcs2	**HMG CoA-S2**	1.00 ± 0.06	0.99 ± 0.06
Sqle	**SQLE**	1.00 ± 0.20	1.07 ± 0.21
Idi1	**IDI1**	1.00 ± 0.10	**1.30 ± 0.10***
Fdps	**FDPS**	1.00 ± 0.23	1.21 ± 0.17
Fdft1	**FDFT1**	1.00 ± 0.09	0.87 ± 0.14
Cholesterol excretion			
Abcg5	**ABCG5**	1.00 ± 0.10	0.82 ± 0.09
Abcg8	**ABCG8**	1.00 ± 0.07	0.83 ± 0.12
HDL metabolism			
Apoa1	**ApoA1**	1.00 ± 0.10	0.96 ± 0.15
Lipe	**HL**	1.00 ± 0.30	0.70 ± 0.16
Pltp	**PLTP**	1.00 ± 0.11	**0.78 ± 0.10***
Abca1	**ABCA1**	1.00 ± 0.07	**0.78 ± 0.09***
Lcat	**LCAT**	1.00 ± 0.04	**0.87 ± 0.06***
CETP	**CETP**	1.00 ± 0.17	0.73 ± 0.20

SUPPLEMENTARY TABLE 4 - **Effect of metformin on BAT expression of genes involved in tissue differentiation, lipoprotein/FA uptake, TG synthesis, FA oxidation and mitochondrial functions.** Brown adipose tissues were isolated from 4 h-fasted mice treated with or without metformin for 4 weeks. mRNA expression of the indicated genes were quantified by RT-PCR relative to CypD gene and expressed as fold difference compared with the control group. Data are means +/- SEM (n=7-8).

Genes by function	Protein	Fold change	
		Control	Metformin
BAT differentiation			
Prdm16	**PRDM16**	1.00 ± 0.27	1.14 ± 0.35
Cidea	**CIDEA**	1.00 ± 0.20	1.09 ± 0.20
Dio2	**DIO2**	1.00 ± 0.16	1.00 ± 0.20
Essra	**ESSR**α	1.00 ± 0.36	1.03 ± 0.43

Genes by function	Protein	Fold change	
		Control	Metformin
Lipoprotein/FA uptake			
CD36	**CD36**	1.00 ± 0.11	0.90 ± 0.12
Ldlr	**LDLr**	1.00 ± 0.20	1.19 ± 0.29
Lrp1	**LRP1**	1.00 ± 0.09	1.34 ± 0.34
Vldlr	**VLDLr**	1.00 ± 0.12	0.96 ± 0.11
Gpihbp1	**GPIHBP1**	1.00 ± 0.05	1.17 ± 0.13
Lpl	**LPL**	1.00 ± 0.16	0.96 ± 0.22
FA/TG synthesis			
Scd1	**SCD1**	1.00 ± 0.17	0.94 ± 0.26
Fasn	**FAS**	1.00 ± 0.14	1.25 ± 0.22
Acly	**ACLY**	1.00 ± 0.23	0.94 ± 0.18
Dgat1	**DGAT1**	1.00 ± 0.16	1.10 ± 0.13
Pck1	**PEPCK**	1.00 ± 0.18	1.18 ± 0.26
Gpam	**GPAT**	1.00 ± 0.23	1.03 ± 0.31
FA oxidation			
Ppara	**PPARα**	1.00 ± 0.23	1.15 ± 0.25
Pparg	**PPARγ**	1.00 ± 0.06	1.06 ± 0.08
Cpt1a	**CPT1α**	1.00 ± 0.20	0.98 ± 0.31
Prkaa1	**AMPKα1**	1.00 ± 0.12	1.11 ± 0.14
Prkaa2	**AMPKα2**	1.00 ± 0.20	1.09 ± 0.14
Acaca	**ACC1**	1.00 ± 0.19	1.12 ± 0.19
Acacb	**ACC2**	1.00 ± 0.19	1.25 ± 0.26
Lipid droplets			
Cidea	**CIDEA**	1.00 ± 0.20	1.09 ± 0.20
Cidec	**FSP27**	1.00 ± 0.23	1.05 ± 0.28
Pnpla2	**ATGL**	1.00 ± 0.24	1.04 ± 0.36
Plin2	**ADRP/Perilipin 2**	1.00 ± 0.13	1.03 ± 0.16
Plin4	**S3–12/Perilipin 4**	1.00 ± 0.17	0.94 ± 0.19
Plin5	**PAT-1/Perilipin 5**	1.00 ± 0.23	1.04 ± 0.31
Mitochondria			
Pparagc1a	**PGC1α**	1.00 ± 0.25	1.01 ± 0.21
Tfam	**Tfam**	1.00 ± 0.13	0.96 ± 0.17
Cs	**CS**	1.00 ± 0.19	0.96 ± 0.24
Ucp1	**UCP1**	1.00 ± 0.12	1.13 ± 0.05
Cox7a1	**COX7**	1.00 ± 0.11	1.05 ± 0.07
Atp5a1	**ATP5A1**	1.00 ± 0.09	0.99 ± 0.09
Ndufb8	**NDUFB8**	1.00 ± 0.13	0.98 ± 0.13
Sdha	**SDHA**	1.00 ± 0.10	1.06 ± 0.21
Sdhb	**SDHB**	1.00 ± 0.12	0.90 ± 0.10
Uqcrc2	**UQCRC2**	1.00 ± 0.08	1.04 ± 0.07

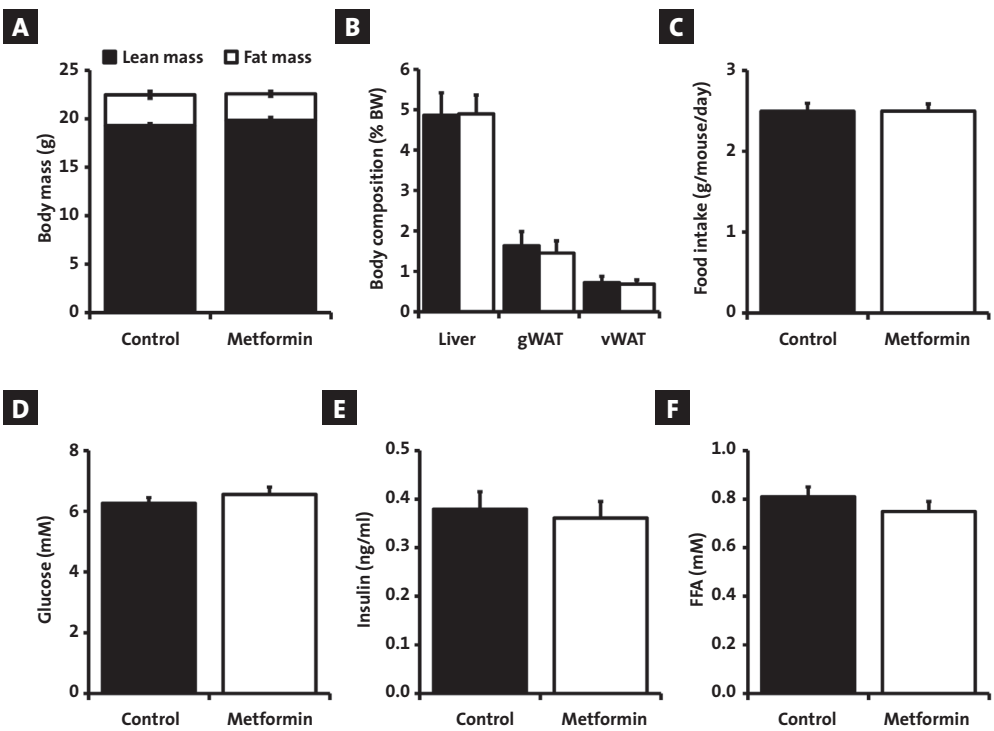

SUPPLEMENTARY FIGURE 1 - Effect of metformin on body weight and composition, food intake and various plasma parameters. Body weight and composition **A-B** and mean food intake **C** were measured throughout the study in control (black bars) and metformin-treated (open bars) mice. Blood samples were collected as described in **FIGURE 1** and plasma glucose **D**, insulin **E** and free fatty acids (FFA; **F** levels were determined.
Values are means ± SEM (n=9/group).

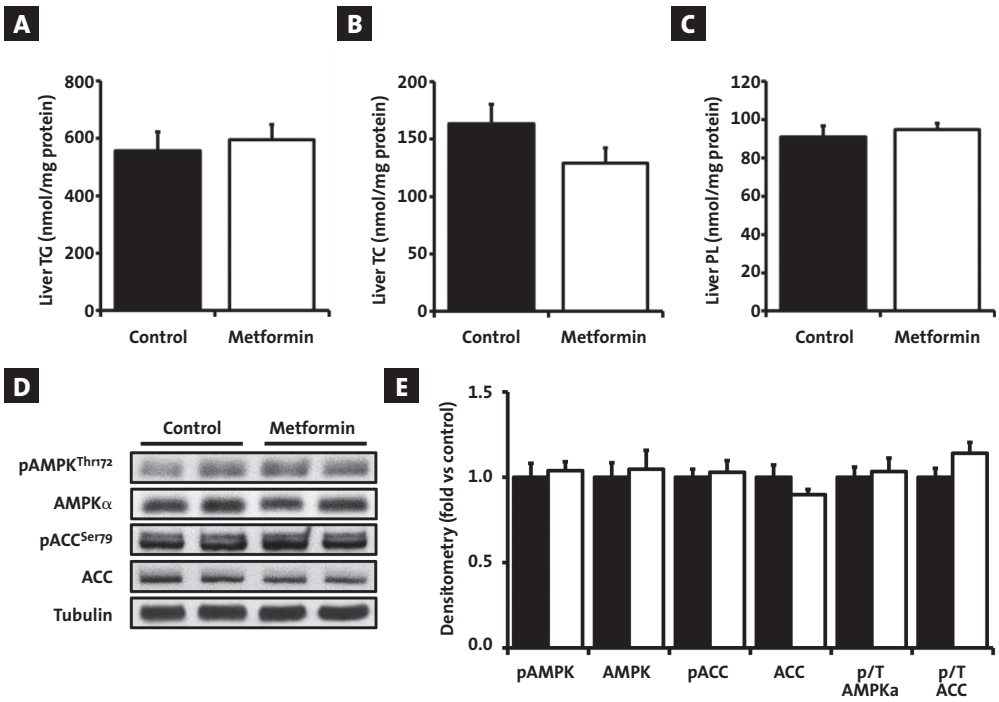

SUPPLEMENTARY FIGURE 2 - Effect of metformin on hepatic lipid composition and AMPK signalling. Livers from 4 h-fasted mice were collected after 4 weeks of treatment with (open bars) or without metformin (control, black bars) and immediately snap-frozen in liquid nitrogen. Hepatic TG **A**, TC **B** and PL **C** content were measured after lipid extraction. The phosphorylation state of Thr172-AMPK and Ser79-ACC, and AMPKα and ACC protein expression were assessed by Western blot **D**, followed by densitometric quantification **E**. Tubulin expression was used as internal housekeeping protein. Data are means ± SEM (n=5-8 per group).

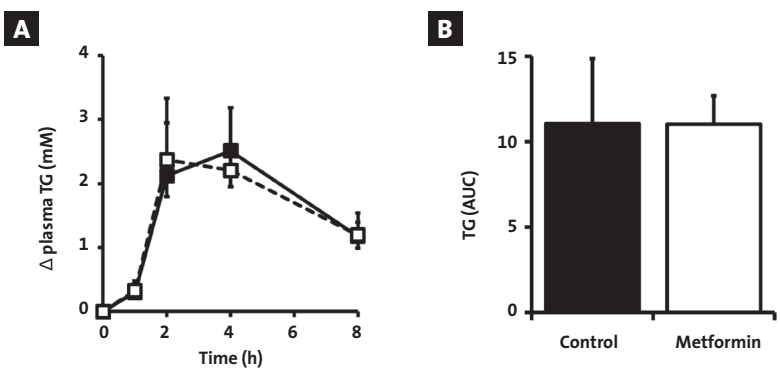

SUPPLEMENTARY FIGURE 3 - Effect of metformin on postprandial TG response. Overnightfasted control (closed squares) and metformin-treated (open squares) mice were given an intragastric bolus of 200 µl of olive oil. Blood samples were drawn at 0, 1, 2, 4, and 8 h. TG concentrations were determined in plasma and corrected for their respective values at time 0 **A**. The areas under the curse were calculated **B**. Data are means ± SEM (n=9-10/group).